

Article

# Optimal Unit Commitment and Generation Scheduling of Integrated Power System with Plug-In Electric Vehicles and Renewable Energy Sources

Vikram Kumar Kamboj <sup>1,2,3</sup> and Om Parkash Malik <sup>2,\*</sup> 

<sup>1</sup> School of Electronics and Electrical Engineering, Lovely Professional University, Phagwara 144001, India; vikram.kumar@ucalgary.ca

<sup>2</sup> Schulich School of Engineering, University of Calgary, Calgary, AB T2N 1N4, Canada

<sup>3</sup> Bisset School of Business, Mount Royal University, Calgary, AB T3E 6K6, Canada

\* Correspondence: maliko@ucalgary.ca

**Abstract:** The integration of wind energy sources and plug-in electric vehicles is essential for the efficient planning, reliability, and operation of modern electric power systems. Minimizing the overall operational cost of integrated power systems while dealing with wind energy sources and plug-in electric vehicles in integrated power systems using a chaotic zebra optimization algorithm (CZOA) is described. The proposed system deals with a probabilistic forecasting system for wind power generation and a realistic plug-in electric vehicle charging profile based on travel patterns and infrastructure characteristics. The objective is to identify the optimal scheduling and committed status of the generating unit for thermal and wind power generation while considering the system power demand, charging, and discharging of electric vehicles, as well as power available from wind energy sources. The proposed CZOA adeptly tackles the intricacies of the unit commitment problem by seamlessly integrating scheduling and the unit's committed status, thereby enabling highly effective optimization. The proposed algorithm is tested for 10-, 20-, and 40-generating unit systems. The empirical findings pertaining to the 10-unit system indicate that the amalgamation of a thermal generating unit system with plug-in electric vehicles yields a 0.84% reduction in total generation cost. Furthermore, integrating the same system with a wind energy source results in a substantial 12.71% cost saving. Notably, the integration of the thermal generating system with both plug-in electric vehicles and a wind energy source leads to an even more pronounced overall cost reduction of 13.05%. The outcome of this study reveals competitive test results for 20- and 40-generating unit systems and contributes to the advancement of sustainable and reliable power systems, fostering the transition towards a greener energy future.

**Keywords:** CZOA; electric vehicle; UCP; wind power



**Citation:** Kamboj, V.K.; Malik, O.P. Optimal Unit Commitment and Generation Scheduling of Integrated Power System with Plug-In Electric Vehicles and Renewable Energy Sources. *Energies* **2024**, *17*, 123. <https://doi.org/10.3390/en17010123>

Academic Editor: Javier Contreras

Received: 16 November 2023

Revised: 17 December 2023

Accepted: 19 December 2023

Published: 25 December 2023



**Copyright:** © 2023 by the authors. Licensee MDPI, Basel, Switzerland. This article is an open access article distributed under the terms and conditions of the Creative Commons Attribution (CC BY) license (<https://creativecommons.org/licenses/by/4.0/>).

## 1. Introduction

Unit commitment is a critical component of the operation and scheduling of electric power systems. It involves determining the optimal schedule and committed status of power generation units to meet the forecasted electricity demand at the minimum cost while satisfying various operational constraints. Unit commitment plays a vital role in ensuring the reliable and efficient operation of power systems, as it determines the commitment and dispatch of power generation resources over a specified time horizon.

The unit commitment problem is characterized by its complexity due to numerous factors, including variability and uncertainty in electricity demand, the availability of different types of power generation units (such as thermal, hydro, wind, and solar), transmission constraints, and the consideration of environmental constraints and economic factors. Solving the unit commitment problem requires sophisticated optimization techniques

and algorithms to find the best combination of committed units and their corresponding generation schedules.

Traditionally, unit commitment was solved using deterministic methods that assumed perfect knowledge of future demand and system conditions. However, with the increasing integration of renewable energy sources and the growing adoption of demand response programs, the unit commitment problem has become more challenging. The variability and uncertainty associated with renewable energy generation and demand response participation require the consideration of probabilistic approaches and advanced forecasting techniques in unit commitment solutions.

Moreover, the transition towards a greener and more sustainable energy future has introduced new complexities in unit commitment. The integration of intermittent renewable energy sources, such as wind and solar power, requires the careful coordination of generation schedules to accommodate their inherent variability and intermittent nature. Additionally, the emergence of plug-in electric vehicles (PEVs) as a potential distributed energy resource adds another dimension to the unit commitment problem, as the charging and discharging patterns of PEVs need to be considered in the optimization process.

Highly effective unit commitment algorithms and techniques wield substantial influence over the operational and planning aspects of power systems. They empower system operators and planners to make informed decisions, thereby guaranteeing a dependable and economically efficient power supply that integrates renewable energy sources, demand response programs, and emerging technologies. This paper endeavors to delve into and put forward advanced optimization methods for determining the unit commitment problem, taking into consideration the complexities and challenges involved in modern power systems.

The major findings of the available literature on the unit commitment of integrated power systems are summarized in Table 1.

**Table 1.** Literature Review.

Sr. No.	Paper Title	Year	Main Finding
1.	Integration of Renewable and Electric Vehicles in Power System: Review [1]	2023	This paper presents a comprehensive review of integrating Renewable Energy Sources (RESs) and Electric Vehicles (EVs) into power systems, emphasizing the sustainable approach to address environmental impacts. It highlights the implications of widespread EV adoption for power system management and categorizes the reviewed literature based on primary objectives, such as emissions reduction and EV charging infrastructure [1].
2.	A New hybrid optimization algorithm for multi-objective optimal power flow in an integrated WE, PV, and PEV power system [2]	2023	This study proposes a novel hybrid multi-objective evolutionary algorithm (MOEA) for the optimal power flow (OPF) problem in transmission networks. It integrates wind energy (WE), photovoltaic (PV), and plug-in electric vehicle (PEV) systems' uncertainty, using adaptive penalty computation and selection features using the invasive weed optimization (IWO) method. The suggested method is evaluated on IEEE 57 and IEEE 118-bus systems, demonstrating its viability and superiority through a one-way ANOVA test [2].
3.	Optimal Sizing of Hybrid Renewable Energy System for Electricity Production for Remote Areas [3]	2022	This study explores the adoption of alternative energy resources, specifically hybrid renewable energy systems, to meet the electrical load demand of a remote site in India. Two intelligent approaches, Improved Harmony Search (IHS) and Particle Swarm Optimization (PSO), are used to optimize the system and minimize the Net Present Cost (NPC) [3].

Table 1. Cont.

Sr. No.	Paper Title	Year	Main Finding
4.	A Review on the unit Commitment Problem-Approaches, Techniques and Resolution Methods [4]	2022	This paper presents a review of the unit commitment problem, focusing on techniques for optimizing thermal generators' schedules in power systems. It addresses the significance of the unit commitment problem in handling emerging energy market trends, such as renewable energy integration and non-conventional energy storage [4].
6.	A unit commitment Model Considering Peak Regulation of Units for Wind Power Integrated Power System [5]	2020	This paper introduces a new unit commitment model to tackle the challenges of peak regulation in power systems with high wind power penetration. The model incorporates regular peak regulation, deep peak regulation, and deep peak regulation with oil operation stages of units. It effectively addresses net load fluctuations by scheduling peak power regulation capacity and peak ramp regulation capability to meet power capacity and ramp capability demands [5].
7.	A New solution to Profit Based Unit Commitment Problem Considering PEVs/BEVs and Renewable Energy Sources [6]	2020	This paper focuses on the unit commitment problem in the power sector, considering dynamic load demand and the inclusion of electric vehicles. The proposed mathematical formulation uses Intensify Harris Hawks Optimizer (IHHO) to find the most economical patterns of generating stations, meeting varying load demand with minimum production cost and higher reliability. The study also emphasizes the importance of renewable energy sources to generate low-cost power with reduced environmental impact, considering the effects of increasing industrialization on the environment [6].

This paper is structured as follows: problem formulation is under Section 2, the chaotic zebra optimization algorithm is explained in Section 3, test systems are described in Section 4, results and discussion are given in Section 5, and finally Section 6 focuses on the conclusions and future scope of the research work. In this paper, the chaotic zebra optimization algorithm has been tested to determine the optimal generating cost of an integrated power system of 10-, 20-, and 40-generating units systems.

## 2. Problem Formulation

The unit commitment problem (UCP) is a crucial optimization challenge in power systems that involves determining the optimal schedule of operation for a set of power generation units over a specified time horizon. When integrated with wind energy systems and plug-in electric vehicles (PEVs), the objective function becomes more complex to account for the intermittent and uncertain nature of wind power as well as the dynamic nature of PEV charging and discharging. The overall goal is to find the optimal schedule for the power generation units, including wind power, and the charging and discharging of electric vehicles to minimize the total operating cost while satisfying various constraints such as demand, power generation limits, and system stability. The objective function for the unit commitment problem integrated with a wind energy system and plug-in electric vehicles is illustrated in Equation (1) [1–5].

$$\text{Min OGC} = \sum_{g=1}^{NG} \sum_{h=1}^{NH} [(a_g P_{g,h}^2 + b_g P_{g,h} + c_g) U_{g,h} + SUC_g \{U_{g,h}(1 - U_{g,(h-1)})\} + SDC_g \{U_{g,h}(1 - U_{g,(h-1)})\}] + \sum_{h=1}^{NH} C_h^{PEV} + \sum_{h=1}^{NH} C_h^{WIND} \quad (1)$$

where  $SUC_g$  and  $SDC_g$  are the start-up and shut-down costs, respectively, for generating unit 'g'. OGC indicates the overall generation cost of the system. Mathematically, the start-up cost is given by Equation (2).

$$SUC_{gh} = \begin{cases} HSC_g; & \text{for } MDT_g \leq MDT_g^{ON} \leq (CSH_g + MDT_g) \\ CSC_g; & \text{for } MDT_g^{ON} \geq (MDT_g + CSH_g) \end{cases} \quad (2)$$

$(g \in NG; h = 1, 2, 3 \dots NH)$

here,  $HSC_g$  and  $CSC_g$  indicate a hot start-up and a cold start-up for the  $g^{\text{th}}$  unit, respectively.  $MDT_g^{ON}$  indicates the number of hours the  $g^{\text{th}}$  unit has been in running condition since it was turned on.  $(a_g P_{g,h}^2 + b_g P_{g,h} + c_g)$  represent the fuel cost of the unit. Equation (1) is subject to the following system constraints:

- System power balance constraint

In Equation (3), power demand must be equal to power generated at scheduled hours. Here, power generated from thermal units and plug-in electric vehicles charging and discharging is considered [2].

$$\sum_{\forall g \in NG} P_g \mp \sum_{\forall g \in PEV} P_g^{PEV} = P_g^D \quad (3)$$

$P_g^{PEV} = +P_g^{PEV}$  during the discharging period, and  $P_g^{PEV} = -P_g^{PEV}$  during the charging period.

- System spinning reserve constraint

A proper system spinning reserve is required for the reliable and stable operation of the system [7]. The system spinning reserve requirement is represented as:

$$\sum_{g=1}^{NG} P_g^{\max} + \sum_{g=1}^{NPEV} P_g^{PEV} \geq P_h^D + SR_h \quad (4)$$

- Maximum and minimum power generation limit

For reliable and stable operation, it is necessary that the generating unit should be operated within the defined limit, i.e., the minimum and maximum power generation limit, so that the system continuously supplies the demand. Power generation limit is represented as:

$$P_g^{\min} \leq P_{g,h} \leq P_g^{\max} \quad (5)$$

- Minimum up (MUT)/minimum down time (MDT)

The MUT/MDT of generating units plays a crucial role in the unit commitment problem (UCP). The minimum up and down time is useful in the operation of generating units within this time frame. It puts the limit to the generating unit operation to operate within this minimum up and minimum down time for the system. The minimum up and minimum down time for the generating unit system are illustrated as:

$$T_{on,g}^h \geq MUT_g \quad (6)$$

- Up/down ramp constraint

Ramp-up constraint refers to the rate at which a power-generating unit can increase its output from a lower level to a higher level within a specified time frame; the ramp-down constraint, on the other hand, is the opposite of the ramp-up constraint. It specifies the rate at which a power-generating unit can decrease its output from a higher level to a lower level within a given time frame. The ramp-up and ramp-down of unit g for scheduled hours h is given by the below equation:

$$RU_g \geq P_{gh} - P_{g(h-1)}$$

$$RD_g \geq P_{g(h-1)} - P_{gh} \quad (7)$$

- Vehicle balance constraint

The vehicle balance for the system is described as [2]:

$$\sum_{h=1} N_{V2G}(h) = N_{V2G}^{\max} \quad (8)$$

here,  $V2G$  means vehicle to grid for  $h$  hours, and  $N$  indicates the number of vehicles.

A probabilistic forecasting system for wind power generation has been developed by analyzing historical wind data to model probability distributions and incorporating weather forecasts. For realistic plug-in electric vehicle (PEV) charging profiles, travel patterns and infrastructure characteristics have been considered by leveraging data on commuting habits, charging station locations, and charging behaviors. Integrating these probabilistic models can enhance the accuracy of predictions for both wind power generation and PEV charging, enabling more effective planning and management in an integrated power system [2].

### 3. Chaotic Zebra Optimization Algorithm

The proposed chaotic zebra optimization algorithm (CZOA) is an improved version of the bio-inspired metaheuristic Zebra Optimization Algorithm (ZOA) [8] that mimics the natural behavior of zebras and Chaos. Chaos is a deterministic, random-like technique in nonlinear, non-periodic, non-converging, and limited dynamical systems. It uses chaotic variables, making it faster than stochastic searches. Chaos can generate repeatable and predictable sequences by changing its starting state, and it is sensitive to changes in parameters and conditions. Different chaotic maps are used in optimization tasks. In the proposed research, the Chebyshev chaotic map has been used to improve the exploitation search capability of existing ZOA in local search space. The mathematical function of the Chebyshev chaotic map can be described by Equation (9):

$$r_{k+1} = \cos(k \cos^{-1}(r_k)) \quad (9)$$

where  $r_{k+1}$  is the chaotic variable generated through Chebyshev chaotic map.

The incorporation of a Chaotic Chebyshev map in algorithms theoretically enhances efficiency and convergence behavior. Leveraging chaotic dynamics, the map promotes a balanced exploration–exploitation strategy, preventing premature convergence to local optima. The chaotic and pseudorandom nature of the map aids in escaping regular patterns, fostering global search capabilities, and diversifying the solution space. This adaptability accelerates convergence speed by dynamically responding to optimization challenges, contributing to the algorithm’s ability to efficiently navigate complex landscapes and converge towards optimal solutions.

In the proposed algorithm, zebra replicates the foraging pattern of zebras and their defensive responses to predator attacks. The zebras are first placed in a random location inside the search area. ZOA uses population matrices (Equation (10)) to represent the population numerically [8].

$$Z = \begin{bmatrix} Z_1 \\ Z_i \\ Z_N \end{bmatrix}_{N \times m} = \begin{bmatrix} z_{1,1} & z_{1,j} & z_{1,m} \\ \dots & \dots & \dots \\ z_{i,1} & z_{i,j} & z_{i,m} \\ \dots & \dots & \dots \\ z_{N,1} & z_{N,j} & z_{N,m} \end{bmatrix}_{N \times m} \quad (10)$$

Each zebra symbolizes a potential answer to the optimization issue. The recommended values of each zebra for the problem variables may thus be used to assess the objective

function. Equation (11) is used to provide the values acquired for the objective function as a vector.

$$F = \begin{bmatrix} F_1 \\ F_i \\ F_N \end{bmatrix}_{N \times 1} = X = \begin{bmatrix} F(Z_1) \\ F(Z_i) \\ F(Z_N) \end{bmatrix}_{N \times 1} \quad (11)$$

where  $F$  is the vector of objectives and is the objective obtained for the zebra.

- **Phase 1: Foraging Behavior**

Zebras may spend between 60 and 80 percent of their time eating, depending on the quality and quantity of vegetation. The best population member is known as the pioneer zebra in ZOA and directs other population members to its location in the search space. Therefore, using Equations (12) and (13), it is possible to quantitatively predict how zebras' positions change throughout the foraging phase.

$$z_{i,j}^{new,P1} = z_{i,j} + r(PZ_j - Iz_{i,j}) \quad (12)$$

- **Phase 2: Defense Strategies against Predators**

Zebras face threats from lions, cheetahs, leopards, wild dogs, brown hyenas, and spotted hyenas. They also face crocodiles when approaching water. When attacked by smaller predators, zebras become more aggressive. The ZOA design predicts either an escape route or an aggressive course of action.

In the first approach, when lions attack zebras, the zebras flee the area where they are situated to avoid the lion's onslaught. Mathematically, this tactic may be represented by mode  $S_1$  in Equation (13). The other zebras in the herd migrate towards the attacked zebra in the second method when other predators attack one of the zebras to intimidate and confuse the predator by erecting a protective structure. Zebras' behavior is mathematically represented by mode  $S_2$  in Equation (13).

$$Z_{i,j}^{new,P2} = \begin{cases} S_1 : z_{i,j} + R(2r - 1) \\ (1 - \frac{t}{T})z_{i,j}; & Ps \leq 0.5 \\ S_2 : z_{i,j} + r(AX_j - Iz_{i,j}); & else \end{cases} \quad (13)$$

Zebras' positions are updated, and the new location is approved for a zebra if it has a higher value for the goal function. This updating condition is represented as:

$$Z_i = \begin{cases} Z_i^{new,P2}, F_i^{new,P2} < F_i; \\ Z_i, & else, \end{cases} \quad (14)$$

The Zebra Optimization Algorithm faces a research gap in scalability and adaptation to complex optimization landscapes. To address this, a Chaotic Chebyshev map is proposed to improve the algorithm's efficiency and convergence behavior. This variant aims to bridge the gap and provide practical solutions for complex optimization landscapes by utilizing the chaotic dynamics of the sinusoidal map. The PSEUDO code of the proposed optimizer is shown in Algorithm 1.

The Chaotic Zebra Optimization Algorithm plays a key role in minimizing the overall operational cost of an integrated power system by leveraging chaotic dynamics for the efficient exploration and exploitation of the solution space. CZOA enhances the search process, allowing for the optimal scheduling of power generation units, including wind energy and plug-in electric vehicles, to achieve cost reductions. Its chaotic nature enables adaptability, aiding in escaping local optima and promoting convergence to global optimal solutions, thus contributing to improved operational cost minimization in the integrated power system.

**Algorithm 1.** PSEUDO code of CZOA

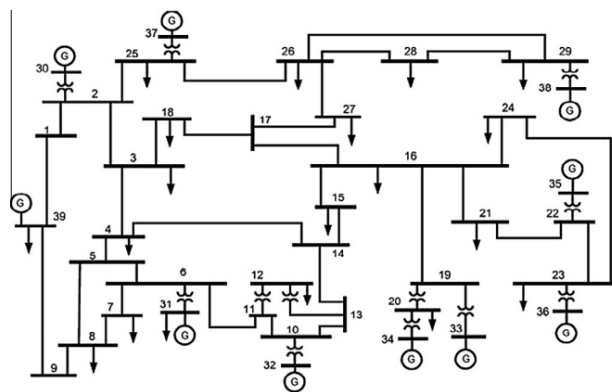
---

**Inputs:** Search Agents, T, LB, UB, dimensions  
**Initialize** X matrix with random values within bounds for each element  
**Initialize** fit array with fitness values for each agent  
**Initialize**  $F_{best}$  and PZ  
**for** t = 1 to Max\_iterations:  
    **Update**  $F_{best}$  and PZ based on fit values  
    **for** i = 1 to Search Agents  
        **Choose** a strategy I = round(1 + rand())  
        **if** I == 1:  
            **Calculate**  $z_{i,j}^{new,P1}$  based on foraging behavior using Equation (12)  
        **else:**  
        **Choose** an attacking predator AZ based on certain conditions  
        **Calculate**  $Z_i^{new,P2}$  based on defense behavior using Equation (13)  
        **Apply** bounds to  $z_{i,j}^{new,P1}$  or  $Z_i^{new,P2}$   
        **Calculate** fitness  $F_i^{new,P2}$   
        **if**  $F_i^{new,P2} \leq F_i$ :  
            **Update**  $z(i, \cdot)$  and  $F_i$  using Equation (14)  
    **Store** the best-so-far solution and other performance metrics  
**Return** Best Position, Best fitness and convergence curve

---

**4. Test Systems**

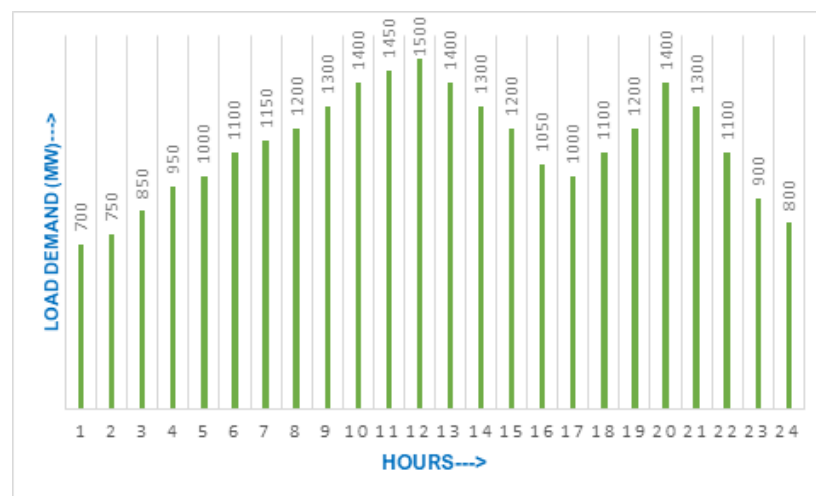
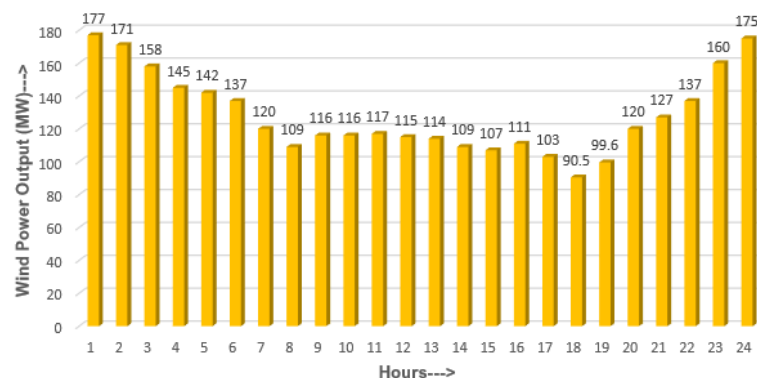
The effectiveness of the proposed algorithm has been tested on 10-, 20-, and 40-generating unit systems. Test data for the 10-generating unit test system have been taken from IEEE 39-bus system [9]. The single line diagram for the IEEE-39 bus system is shown in Figure 1, and its generating units characteristics, i.e., fuel cost coefficients, minimum and maximum power generating limit, minimum up time, minimum down time, start-up costs, cold start hours and initial status of each generating units, are given in Table 2. The load demand profile for 24 h for the 10-unit system is shown in Figure 2. To obtain the 20-unit test system, the 10-unit system was duplicated, and the load demand was doubled. For the 40-unit test system, the 10-unit system was quadrupled, and load demand was accordingly multiplied by four. The 10-unit test system data were scaled appropriately for the problem with 20- and 40-unit test systems. The day-ahead forecast wind power output is shown in Figure 3 [10]. To analyze the impact of PEVs, a fleet of 40,000 vehicles was taken into consideration with each vehicle having a battery capacity of 15 kW. Further, it was assumed that only 20% of the vehicles were involved in charging and discharging, the departure state of charge ( $\delta$ ) was 50%, and efficiency ( $\eta$ ) was 85%. Therefore, the study involved up to 8000 vehicles, with both charge and discharge operations collectively amounting to 51 MW of power. The spot price for the charging and discharging of vehicles is taken from [11].



**Figure 1.** Single line diagram of 10-generating unit system (IEEE 39 bus system) Reproduced with permission from [9], Elsevier, 2023.

**Table 2.** Test data for IEEE 39 bus system (10-generating unit system) [9].

Unit Parameter	U1	U2	U3	U4	U5	U6	U7	U8	U9	U10
$P_g^{\max}$ (MW)	455	455	130	130	162	80	85	55	55	55
$P_g^{\min}$ (MW)	150	150	20	20	25	20	25	10	10	10
$c_g$ (\$/hour)	1000	970	700	680	450	370	480	660	665	670
$b_g$ (\$/MWh)	16.19	17.26	16.60	16.50	19.70	22.26	27.74	25.92	27.27	27.79
$a_g$ (\$/MWh <sup>2</sup> )	0.00048	0.00031	0.002	0.00211	0.00398	0.00712	0.00079	0.00413	0.00222	0.00173
$MUT_g$ (h)	8	8	5	5	6	3	3	1	1	1
$MDT_g$ (h)	8	8	5	5	6	3	3	1	1	1
$HSC_g$ (\$)	4500	5000	550	560	900	170	260	30	30	30
$CSC_g$ (\$)	9000	10,000	1100	1120	1800	340	520	60	60	60
$CSH_g$ (h)	5	5	4	4	4	2	2	0	0	0
$IS_g$	8	8	-5	-5	-6	-3	-3	-1	-1	-1

**Figure 2.** Load demand profile for 10-generating unit system [9].**Figure 3.** Day-ahead forecast wind power output [10].

## 5. Results and Discussion

To comprehensively evaluate the proposed Chaotic Zebra Optimization Algorithm, it is imperative to explore its effectiveness relative to other optimization techniques. Integrating benchmark algorithms such as Genetic Algorithms, Grey Wolf Optimizer, or Simulated Annealing can provide a comparative framework. Assessing solution quality, convergence speed, and computational efficiency across diverse optimization problems would offer insights into CZOA's robustness. A systematic comparison, identifying scenarios where CZOA excels or where alternative algorithms may outperform, can validate its efficacy. This approach enhances the credibility of CZOA by establishing its competitiveness within

a broader context, contributing to a more thorough understanding of its strengths and limitations in diverse optimization landscapes.

The proposed algorithm has been tested on MATLAB 2021a using an Intel(R) Core (TM) i7-5600U CPU @ 2.60 GHz 2.60 GHz processor with 16 GB RAM. The performance and effectiveness of the optimizer have been tested on 10-, 20-, and 40-generating unit systems for 30 trial solutions, and a statistical analysis of the optimizer has been performed using the Wilcoxon rank sum test and *t*-test. The best, mean, worst, std, median, and *p*-values are recorded for the effective analysis and validation of the results. The performance of the proposed CZOA algorithm has been initially tested on CEC2005 unimodal benchmark problems, and its validation has been performed by comparing the results with well-known optimizers White Shark Optimizer (WSO) [12], Marine Predators Algorithm (MPA) [13], Whale Optimizer Algorithm(WOA) [14], Grey Wolf Optimizer (GWO) [15], Gravitational Search Algorithm (GSA) [16], Teaching-Learning Based Optimizer (TLBO) [17], and Genetic Algorithm(GA) [18] (Table 3). The results for the 10-generating unit system for a conventional thermal system and a thermal system integrated with Wind and PEVs system, the results for the 20-generating unit system, and the corresponding results for 40-generating units are depicted in Tables 4–6, respectively. The commitment and generating schedule for the 10-generating unit system for an integrated power system is shown in Tables 7 and 8. The generation schedule for the 20-unit test system is shown in Tables 9 and 10, and the overall results for the 40-generating unit system for different scenarios are presented in Table 11. In summary, integrating wind, solar, and PEVs into the 40-generating unit system consistently improves overall performance, with statistical tests confirming the significance of these enhancements. The table also provides insights into the variability and computational times associated with each scenario.

**Table 3.** Test results of CZOA for CEC 2005 unimodal benchmark problems.

Functions	Index	CZOA	WSO [9]	MPA [10]	WOA [11]	GWO [12]	GSA [13]	TLBO [14]	GA [15]
F1	Mean	$3.2 \times 10^{-258}$	65.84207	$1.92 \times 10^{-49}$	$1.40 \times 10^{-151}$	$1.77 \times 10^{-59}$	$1.33 \times 10^{-16}$	$2.52 \times 10^{-74}$	30.4715
	Best	$2.3 \times 10^{-261}$	5.289861	$3.80 \times 10^{-52}$	$9.30 \times 10^{-171}$	$1.49 \times 10^{-61}$	$5.35 \times 10^{-17}$	$5.86 \times 10^{-77}$	17.90903
	Worst	$9.5 \times 10^{-258}$	238.6714	$1.66 \times 10^{-48}$	$2.70 \times 10^{-150}$	$7.71 \times 10^{-59}$	$3.73 \times 10^{-16}$	$2.59 \times 10^{-73}$	56.87106
	Std	0	58.09538	$4.33 \times 10^{-49}$	$6.60 \times 10^{-151}$	$2.35 \times 10^{-59}$	$7.88 \times 10^{-17}$	$6.78 \times 10^{-74}$	11.51854
	Median	$5.7 \times 10^{-260}$	45.37455	$4.16 \times 10^{-50}$	$2.20 \times 10^{-159}$	$1.07 \times 10^{-59}$	$1.13 \times 10^{-16}$	$1.69 \times 10^{-75}$	28.17077
F2	Mean	$5.3 \times 10^{-134}$	2.1377	$6.96 \times 10^{-28}$	$2.50 \times 10^{-105}$	$1.35 \times 10^{-34}$	$5.48 \times 10^{-08}$	$6.76 \times 10^{-39}$	2.785606
	Best	$4.1 \times 10^{-137}$	0.661815	$1.84 \times 10^{-29}$	$7.90 \times 10^{-118}$	$4.87 \times 10^{-36}$	$3.48 \times 10^{-08}$	$8.81 \times 10^{-40}$	1.743611
	Worst	$1.6 \times 10^{-133}$	7.438052	$4.70 \times 10^{-27}$	$2.70 \times 10^{-104}$	$7.90 \times 10^{-34}$	$1.23 \times 10^{-07}$	$2.44 \times 10^{-38}$	3.80275
	Std	$9.1 \times 10^{-134}$	1.953299	$1.20 \times 10^{-27}$	$7.60 \times 10^{-105}$	$2.16 \times 10^{-34}$	$2.06 \times 10^{-08}$	$6.14 \times 10^{-39}$	0.599756
	Median	$5 \times 10^{-136}$	1.528931	$3.51 \times 10^{-28}$	$3.40 \times 10^{-108}$	$6.50 \times 10^{-35}$	$5.12 \times 10^{-08}$	$4.97 \times 10^{-39}$	2.738814
F3	Mean	$1.1 \times 10^{-159}$	1784.524	$2.51 \times 10^{-12}$	19,939.26	$2.17 \times 10^{-14}$	475.0243	$3.84 \times 10^{-24}$	2166.814
	Best	$2.4 \times 10^{-167}$	1039.407	$6.18 \times 10^{-19}$	2062.816	$2.35 \times 10^{-19}$	245.7179	$2.20 \times 10^{-29}$	1422.763
	Worst	$3.3 \times 10^{-159}$	3539.57	$1.43 \times 10^{-11}$	34,653.75	$4.04 \times 10^{-13}$	1185.13	$3.60 \times 10^{-23}$	3455.476
	Std	$1.9 \times 10^{-159}$	691.1359	$4.83 \times 10^{-12}$	9420.548	$9.93 \times 10^{-14}$	242.5098	$1.19 \times 10^{-23}$	704.235
	Median	$1.2 \times 10^{-163}$	1556.732	$1.83 \times 10^{-13}$	20,303.94	$4.66 \times 10^{-16}$	399.9344	$4.04 \times 10^{-26}$	2098.599
F4	Mean	$1.9 \times 10^{-115}$	17.2787	$2.98 \times 10^{-19}$	51.76951	$1.23 \times 10^{-14}$	1.234645	$1.83 \times 10^{-30}$	2.826566
	Best	$5.2 \times 10^{-118}$	11.90291	$3.01 \times 10^{-20}$	0.903667	$6.55 \times 10^{-16}$	$9.89 \times 10^{-09}$	$5.81 \times 10^{-32}$	2.214252
	Worst	$4 \times 10^{-115}$	23.8119	$9.60 \times 10^{-19}$	91.61802	$5.73 \times 10^{-14}$	4.922767	$8.11 \times 10^{-30}$	3.988745
	Std	$2 \times 10^{-115}$	3.178756	$2.52 \times 10^{-19}$	32.60275	$1.61 \times 10^{-14}$	1.527107	$2.64 \times 10^{-30}$	0.514049
	Median	$1.7 \times 10^{-115}$	17.75492	$2.58 \times 10^{-19}$	55.36903	$6.34 \times 10^{-15}$	0.906041	$6.52 \times 10^{-31}$	2.780694
F5	Mean	28.68011	10,788.60	23.30066	27.28239	26.55501	44.00585	26.76115	594.79
	Best	28.59876	1345.963	22.78581	26.69534	25.54099	25.85872	25.5631	228.5792
	Worst	28.79517	92,623.17	24.02522	28.70663	27.12889	167.0769	28.72392	2254.801
	Std	0.10245	22,093.25	0.427845	0.636008	0.579436	48.79555	1.030818	467.867
	Median	28.64641	5604.085	23.27164	27.05974	26.20545	26.32007	26.30152	475.0975
F6	Mean	2.067735	100.8059	$1.80 \times 10^{-09}$	0.081492	0.660188	$1.05 \times 10^{-16}$	1.260143	34.11331
	Best	1.99537	16.93604	$8.07 \times 10^{-10}$	0.01051	0.246482	$5.52 \times 10^{-17}$	0.232888	15.59683
	Worst	2.20709	382.1118	$4.80 \times 10^{-09}$	0.326421	1.251026	$1.81 \times 10^{-16}$	2.162628	62.70425
	Std	0.120715	105.1108	$1.03 \times 10^{-09}$	0.111874	0.337545	$4.08 \times 10^{-17}$	0.547394	14.91716
	Median	2.000745	69.50695	$1.60 \times 10^{-09}$	0.031576	0.726589	$9.47 \times 10^{-17}$	1.216208	31.6505
F7	Mean	0.000102	$9.00 \times 10^{-05}$	0.000546	0.001277	0.00083	0.052756	0.001528	0.010578
	Best	$4.1 \times 10^{-05}$	$1.06 \times 10^{-05}$	0.000111	$2.02 \times 10^{-05}$	0.000182	0.01411	$9.00 \times 10^{-05}$	0.003029
	Worst	0.00016	0.000339	0.000898	0.005394	0.001955	0.095479	0.002944	0.021917
	Std	$5.97 \times 10^{-05}$	$9.85 \times 10^{-05}$	0.000236	0.001591	0.000514	0.027476	0.000968	0.005305
	Median	0.000104	$6.37 \times 10^{-05}$	0.000533	0.000817	0.000844	0.05178	0.001505	0.010168



**Table 8.** Generation Schedule of a 10-generating unit system considering a thermal, wind, and PEVs system (SUC is Start-up Cost).

Hours	P <sub>G1</sub>	P <sub>G2</sub>	P <sub>G3</sub>	P <sub>G4</sub>	P <sub>G5</sub>	P <sub>G6</sub>	P <sub>G7</sub>	P <sub>G8</sub>	P <sub>G9</sub>	P <sub>G10</sub>	Power Gen	SUC	Fuel Cost (\$)
H1	405.4	150	0	0	0	0	0	0	0	0	555.4	810	11,208.2886
H2	450.5	150	0	0	0	0	0	0	0	0	600.5	0	11,956.98612
H3	455	258.24	0	0	0	0	0	0	0	0	713.24	560	13,913.71765
H4	455	367.35	0	0	25	0	0	0	0	0	847.35	0	16,763.10377
H5	455	400.99	0	0	25	0	0	0	0	0	880.99	1300	17,351.74272
H6	455	392.24	0	130	25	0	0	0	0	0	1002.24	0	20,059.22509
H7	455	433.54	0	130	25	0	0	0	0	0	1043.54	0	20,782.63555
H8	455	455	0	130	34.67	20	0	0	0	0	1094.67	0	22,169.78975
H9	455	455	0	130	77.24	20	0	0	0	0	1137.24	0	23,027.3795
H10	455	455	130	130	48.52	20	0	0	0	0	1238.52	60	25,339.02043
H11	455	455	130	130	84.77	20	25	0	0	0	1299.77	690	27,246.36959
H12	455	455	130	130	121.27	20	25	0	0	0	1336.27	0	27,995.35102
H13	455	455	130	130	44.27	0	25	0	0	0	1239.27	60	25,609.67163
H14	455	448.53	130	130	25	0	0	0	0	0	1188.53	0	23,937.26184
H15	455	382.02	130	130	25	0	0	0	0	0	1122.02	0	22,772.17488
H16	455	205.81	130	130	25	0	0	0	0	0	945.81	0	19,698.68
H17	455	191.8	130	130	25	0	0	0	0	0	931.8	0	19,455.14054
H18	455	310.06	130	130	25	0	0	0	0	0	1050.06	230	21,514.70663
H19	455	401.61	130	130	25	0	0	0	0	0	1141.61	0	23,115.05718
H20	455	455	130	130	53.04	0	0	10	0	0	1233.04	0	25,531.45645
H21	455	416.42	130	130	25	0	0	0	0	0	1156.42	0	23,374.43344
H22	455	435.56	0	0	25	0	0	0	0	0	915.56	0	17,957.38598
H23	455	249.08	0	0	0	0	0	0	0	0	704.08	0	13,754.17546
H24	430.59	150	0	0	0	0	0	0	0	0	580.59	0	11,626.22282
Total Fuel Cost													489,869.9767

**Table 9.** Generation Schedule of a 20-generating unit system (U1–U10) considering a thermal, wind, and PEVs system.

Hours	P <sub>G1</sub>	P <sub>G2</sub>	P <sub>G3</sub>	P <sub>G4</sub>	P <sub>G5</sub>	P <sub>G6</sub>	P <sub>G7</sub>	P <sub>G8</sub>	P <sub>G9</sub>	P <sub>G10</sub>	P <sub>G11</sub>	P <sub>G12</sub>
H1	455	157	0	0	0	0	0	0	0	0	455	156.5
H2	455	210	0	0	0	0	0	0	0	0	455	209.5
H3	455	316	0	0	0	0	0	0	0	0	455	316
H4	455	358	0	0	0	0	0	0	0	0	455	357.5
H5	455	396	0	0	0	0	0	0	0	0	455	396.5
H6	455	369	0	130	0	0	0	0	0	0	455	369
H7	455	363	130	130	0	0	0	0	0	0	455	362.5
H8	455	406	130	130	25	0	0	0	0	0	455	405.5
H9	455	455	130	130	62	20	0	0	0	0	455	455
H10	455	455	130	130	127	20	25	0	0	0	455	455
H11	455	455	130	130	162	24.5	25	10	0	0	455	455
H12	455	455	130	130	162	65.5	25	10	10	0	455	455
H13	455	455	130	130	128	20	25	0	0	0	455	455
H14	455	455	130	130	65.5	20	0	0	0	0	455	455
H15	455	455	130	130	41.5	0	0	0	0	0	455	455
H16	455	320	130	130	25	0	0	0	0	0	455	319.5
H17	455	274	130	130	25	0	0	0	0	0	455	273.5
H18	455	370	130	130	25	20	0	0	0	0	455	369.8
H19	455	453	130	130	25	20	25	0	0	0	455	452.7
H20	455	455	130	130	132.5	20	25	10	0	0	455	455
H21	455	455	130	130	44	0	25	0	0	0	455	455
H22	455	372	0	130	0	0	0	0	0	0	455	371.5
H23	455	300	0	0	0	0	0	0	0	0	455	300
H24	455	365	0	0	0	20	0	0	0	0	455	0

**Table 10.** Generation Schedule of a 20-generating unit system (U11–U20) considering a thermal, wind, and PEVs system.

Hours	P <sub>G13</sub>	P <sub>G14</sub>	P <sub>G15</sub>	P <sub>G16</sub>	P <sub>G17</sub>	P <sub>G18</sub>	P <sub>G19</sub>	P <sub>G20</sub>	Power Generated	SUC	FC (\$)
H1	0	0	0	0	0	0	0	0	1223	0	24,289.21
H2	0	0	0	0	0	0	0	0	1329	430	26,130.8
H3	0	0	0	0	0	0	0	0	1542	1460	29,841.87
H4	0	130	0	0	0	0	0	0	1755	560	34,152.44
H5	0	130	25	0	0	0	0	0	1858	1450	36,461.94
H6	130	130	25	0	0	0	0	0	2063	0	41,252.05
H7	130	130	25	0	0	0	0	0	2180	0	43,916.52
H8	130	130	25	0	0	0	0	0	2291	1100	46,366.34
H9	130	130	62	0	0	0	0	0	2484	170	50,402.96
H10	130	130	127	20	25	0	0	0	2684	1120	56,227.79
H11	130	130	162	24.5	25	10	0	0	2783	120	59,729.72
H12	130	130	162	65.5	25	10	10	0	2885	120	63,483.43
H13	130	130	128	20	25	0	0	0	2686	0	56,269.22
H14	130	130	65.5	0	0	0	0	0	2491	0	50,544.42
H15	0	130	41.5	0	0	0	0	0	2293	60	45,868.53
H16	0	130	25	0	0	0	0	0	1989	0	40,467.17
H17	0	130	25	0	0	0	0	0	1897	0	38,862.33
H18	0	130	25	0	0	0	0	0	2109.5	0	43,041.32
H19	0	130	25	0	0	0	0	0	2300.4	400	47,121.04
H20	130	130	132.5	20	0	0	0	0	2680	580	56,201.47
H21	130	130	44	20	0	0	0	0	2473	0	50,852.57
H22	130	130	0	20	0	0	0	0	2063	0	41,212.56
H23	130	0	0	0	0	0	0	0	1640	0	32,175.24
H24	130	0	0	0	0	0	0	0	1425	0	27,952.69

**Table 11.** Test results for a 40-generating unit system for different test cases.

Test Case	Best	Average	Worst	STD	Median	Wilcoxon Test	t-Test		Average Time	Worst Time
						p-Value	p-Value	h-Value		
Thermal System	2,246,014	2,250,002	2,252,619	1578.101	2,250,432	$1.73 \times 10^{-6}$	$3.06 \times 10^{-93}$	1	0.043229	0.09375
Thermal + PEVs	2,253,149	2,255,037	2,256,230	859.5718	2,255,440	$1.21 \times 10^{-6}$	$6.40 \times 10^{-101}$	1	0.047917	0.09375
Thermal + SOLAR	2,161,119	2,169,874	2,182,779	8420.975	2,171,364	$1.37 \times 10^{-6}$	$1.08 \times 10^{-71}$	1	0.038021	0.078125
Thermal + WIND	2,171,041	2,174,544	2,178,548	1812.338	2,175,304	$1.56 \times 10^{-6}$	$4.56 \times 10^{-91}$	1	0.042188	0.09375
Thermal + WIND + PEVs	2,166,287	2,169,067	2,171,629	1345.898	2,169,687	$1.29 \times 10^{-6}$	$8.77 \times 10^{-95}$	1	0.039583	0.09375

The Chaotic Zebra Optimization Algorithm effectively addresses the complexities of the unit commitment problem by integrating scheduling decisions with the commitment status of power generation units. By dynamically adjusting the commitment status of units during optimization, CZOA adapts to changing system conditions, optimizing both commitment and scheduling simultaneously. The chaotic nature of CZOA aids in exploring the solution space, ensuring a more comprehensive search for optimal unit commitment strategies that minimize overall operational costs in the integrated power system. A comparison of different case studies for the 10-unit system is presented in Figure 4.

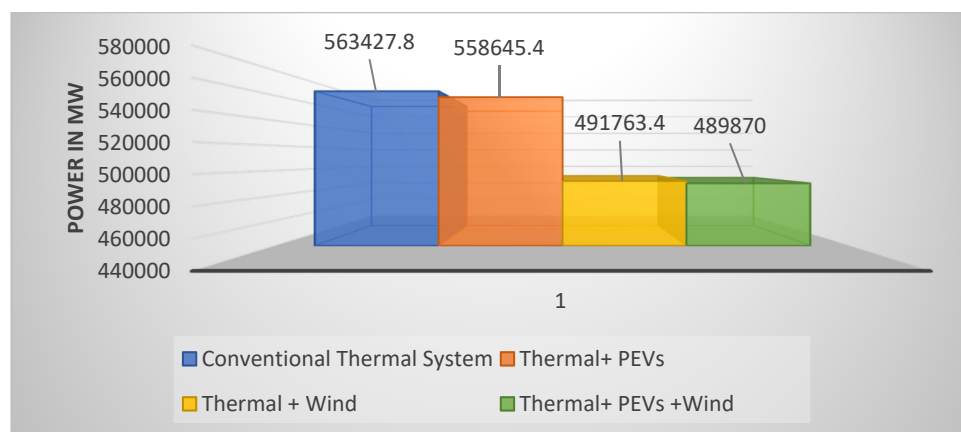


**Figure 4.** Comparison of OGC for different case studies for 10-unit system.

Table 4 compares the performance of a 10-generating unit system in two scenarios: one with only thermal generation and another integrated with wind and plug-in electric vehicles (PEVs). In the “Thermal System”, the best, average, and worst objective function values are higher compared to the integrated scenario, indicating improved system efficiency with wind and PEV integration. The standard deviation and median are also lower in the integrated case, suggesting greater consistency. Computational times for all scenarios are relatively close, with the integrated system showing a slightly longer average time. Statistical tests (Wilcoxon rank sum and *t*-test) reveal highly significant differences in the objective function values between the two scenarios, emphasizing the positive impact of wind and PEV integration on system performance.

Test results for a 20-generating unit system under two different scenarios—one with only thermal generation and another integrated with wind and plug-in electric vehicles (PEVs)—are given in Table 5. In the “Thermal System”, the best, average, and worst objective function values are higher compared to the integrated scenario, indicating enhanced efficiency with wind and PEV integration. The standard deviation and median are slightly higher in the integrated case, suggesting more variability but comparable central tendencies. Computational times are similar between the scenarios, with the integrated system showing a slightly longer average time. The Wilcoxon rank sum and *t*-test indicate highly significant differences in objective function values, affirming the positive impact of wind and PEV integration on the overall system performance for the 20-generating unit setup.

Test results for a 40-generating unit system under two scenarios—a “Thermal System” and one integrated with wind and plug-in electric vehicles (PEVs)—are displayed in Table 6. In the “Thermal + Wind + PEVs” scenario, improvements are evident, with lower best, average, and worst objective function values, indicating increased system efficiency due to wind and PEV integration. The standard deviation and median are lower in the integrated case, suggesting more consistent performance. Computational times are comparable between the scenarios, with the integrated system exhibiting a slightly shorter average time. Both the Wilcoxon rank sum and *t*-tests indicate highly significant differences in objective function values, highlighting the positive impact of wind and PEV integration on the overall system performance for the 40-generating unit system.

Hybrid renewable energy systems play a crucial role in meeting the electrical load demand of remote sites by combining multiple renewable sources such as solar and wind. The integration of diverse sources enhances reliability, ensuring a continuous power supply even in varying weather conditions. Energy storage components, such as batteries, further stabilize power delivery, making these systems efficient and sustainable solutions for off-grid or remote locations with intermittent or no access to the conventional power grid.

Optimizing thermal generators’ schedules in power systems involves adopting advanced techniques such as machine learning, optimization algorithms, and predictive analytics. These approaches consider emerging energy market trends by incorporating

real-time market prices and demand fluctuations. Additionally, to accommodate renewable energy integration, scheduling algorithms must dynamically adjust to the variable nature of renewable sources, ensuring an efficient and balanced utilization of thermal generators alongside intermittent renewables in the evolving energy landscape.

## 6. Conclusions and Future Scope

In conclusion, a novel approach, the Chaotic Zebra Optimization Algorithm (CZOA), aiming to address the critical challenges associated with the integration of wind energy sources and plug-in electric vehicles within modern electric power systems, is presented. The study focuses on optimizing the operation of integrated power systems to minimize overall operational costs while ensuring reliability and efficiency.

Through the implementation of a probabilistic forecasting system for wind power generation and a realistic PEV charging profile based on travel patterns and infrastructure characteristics, the research is aimed at identifying optimal scheduling and committed status for generating units involved in both thermal and wind power generation. Various factors, including the system power demand, charging, and discharging of electric vehicles, as well as the power available from wind energy sources, are considered in this approach.

The proposed CZOA algorithm effectively tackles the complexities of unit commitment problems by seamlessly integrating scheduling and the unit's committed status, ultimately enabling highly effective optimization. The proposed algorithm has been tested rigorously across systems with 10, 20, and 40 generating units, yielding competitive results. Results pertaining to the 10-unit system indicate that the integration of a thermal generating unit system with plug-in electric vehicles yields a 0.84% reduction in total generation costs, while integrating the same system with a wind energy source results in a substantial 12.71% cost saving and the integration of the thermal generating system with both plug-in electric vehicles and a wind energy source leads to an even more pronounced overall cost reduction of 13.05%. The most effective model for achieving operational cost savings involves integrating a thermal power system with both wind energy sources and plug-in electric vehicles.

The average simulation time of the algorithm is high for large-dimension problems. Further study is needed to understand the algorithm's resilience in managing noisy and multimodal functions and its influence on efficient optimization techniques.

The influence of noisy and multimodal functions on the proposed optimization algorithm lies in its ability to navigate complex and unpredictable landscapes. By incorporating chaotic dynamics, the algorithm exhibits resilience to noise, aiding in robust optimization. The multimodal nature is addressed through the algorithm's adaptability, allowing it to explore and exploit multiple solution regions concurrently, enhancing efficiency in finding optimal solutions in challenging, diverse environments.

The Zebra Optimization Algorithm exhibits scalability and adaptation in complex optimization landscapes by efficiently handling an increasing number of decision variables and diverse problem structures. Its ability to dynamically adjust its search strategy enables effective exploration and exploitation, making ZOA well-suited for large-scale optimization problems with intricate and changing characteristics.

**Author Contributions:** Software, V.K.K.; Validation, O.P.M.; Formal analysis, V.K.K. and O.P.M.; Writing—review & editing, O.P.M. All authors have read and agreed to the published version of the manuscript.

**Funding:** This project is sponsored by Mitacs Elevate under application Ref. IT21647 and APC charges are sponsored by Professor O.P. Malik.

**Data Availability Statement:** Data are contained within the article.

**Acknowledgments:** The first author would like to express sincere gratitude to Mitacs and Agam Enterprise for their generous support, which made this research possible. Their commitment to advancing knowledge and innovation has been instrumental in the successful completion of this project.

**Conflicts of Interest:** The authors declare no conflict of interest.

## Nomenclature

$Z$	zebra population
$Z_i$	$i$ th zebra
$z_{i,j}$	$j$ th problem variable proposed by the $i$ th zebra
$N$	No. of zebra population
$m$	No. of decision variables
$Z_{i,j}^{new,P1}$	New status of the $i$ th. zebra based on first phase
$Z_i^{new,P2}$	New status of the $i$ th. zebra based on second phase
$I$	$I$ is the round ( $1 + \text{rand}$ ), $\text{rand}$ is $[0, 1]$ . Thus, $I \in \{1, 2\}$
$T$ and $t$	Maximum number of iterations and iteration counter
$F^{Best}$	Best fitness value
$PZ_j$	Pioneer zebra in $j$ th dimension
$PZ$	Pioneer zebra which is the best member
$r$	Random number in interval $[0, 1]$
$F_i^{new,P2}$	Objective function value in first phase
$F_i^{new,P1}$	Objective function value in second phase
$AZ$	attacked zebras
$R$ and $P_s$	Constant number equal to 0.01 and randomly generated in $[0, 1]$ .
$Z_i^{new,P1}$	New status of the $i$ th. zebra based on first phase

## References

- Manousakis, N.M.; Karagiannopoulos, P.S.; Tsekouras, G.J.; Kanellos, F.D. Integration of Renewable Energy and Electric Vehicles in Power Systems: A Review. *Processes* **2023**, *11*, 1544. [[CrossRef](#)]
- Avvari, R.K.; DM, V.K. A new hybrid evolutionary algorithm for multi-objective optimal power flow in an integrated WE, PV, and PEV power system. *Electr. Power Syst. Res.* **2023**, *214*, 108870. [[CrossRef](#)]
- Kuloor, S.; Hope, G.S.; Malik, O.P. Environmentally constrained unit commitment. *IEE Proc. C (Gener. Transm. Distrib.)* **1992**, *139*, 122–128. [[CrossRef](#)]
- Montero, L.; Bello, A.; Reneses, J. A Review on the Unit Commitment Problem: Approaches, Techniques, and Resolution Methods. *Energies* **2022**, *15*, 1296. [[CrossRef](#)]
- Zhang, X.; Wang, M.; Wang, M.; Jing, L. A Unit Commitment Model Considering Peak Regulation of Units for Wind Power Integrated Power System. In Proceedings of the 2020 IEEE/IAS Industrial and Commercial Power System Asia, I CPS Asia 2020, Weihai, China, 13–15 July 2020; pp. 714–719. [[CrossRef](#)]
- Nandi, A.; Kamboj, V.K. A New Solution to Profit Based Unit Commitment Problem Considering PEVs/BEVs and Renewable Energy Sources. *E3S Web Conf.* **2020**, *184*, 01070. [[CrossRef](#)]
- Imani, M.H.; Yousefpour, K.; Ghadi, M.J.; Andani, M.T. Simultaneous presence of wind farm and V2G in security constrained unit commitment problem considering uncertainty of wind generation. In Proceedings of the 2018 IEEE Texas Power Energy Conference TPEC 2018, College Station, TX, USA, 8–9 February 2018; pp. 1–6. [[CrossRef](#)]
- Trojovska, E.; Dehghani, M.; Trojovský, P. Zebra Optimization Algorithm: A New Bio-Inspired Optimization Algorithm for Solving Optimization Algorithm. *IEEE Access* **2022**, *10*, 49445–49473. [[CrossRef](#)]
- Venkatesan, T.; Sanavullah, M.Y. SFLA approach to solve PBUC problem with emission limitation. *Int. J. Electr. Power Energy Syst.* **2013**, *46*, 1–9. [[CrossRef](#)]
- Zhang, N.; Li, W.; Liu, R.; Lv, Q.; Sun, L. A three-stage birandom program for unit commitment with wind power uncertainty. *Sci. World J.* **2014**, *2014*, 583157. [[CrossRef](#)]
- Saniya, M.; Mohammadi, S. Optimal scheduled unit commitment considering suitable power of electric vehicle and photovoltaic uncertainty. *J. Renew. Sustain. Energy* **2018**, *10*, 043705.
- Braik, M.; Hammouri, A.; Atwan, J.; Al-Betar, M.A.; Awadallah, M.A. White Shark Optimizer: A novel bio-inspired meta-heuristic algorithm for global optimization problems. *Knowl.-Based Syst.* **2022**, *243*, 108457. [[CrossRef](#)]
- Faramarzi, A.; Heidarinejad, M.; Mirjalili, S.; Gandomi, A.H. Marine Predators Algorithm: A nature-inspired metaheuristic. *Expert Syst. Appl.* **2020**, *152*, 113377. [[CrossRef](#)]
- Mirjalili, S.; Lewis, A. The Whale Optimization Algorithm. *Adv. Eng. Softw.* **2016**, *95*, 51–67. [[CrossRef](#)]
- Mirjalili, S.; Mirjalili, S.M.; Lewis, A. Grey Wolf Optimizer. *Adv. Eng. Softw.* **2014**, *69*, 46–61. [[CrossRef](#)]
- Rashedi, E.; Nezamabadi-pour, H.; Saryazdi, S.G. A Gravitational Search Algorithm, Information Sciences. *Inf. Sci.* **2009**, *179*, 2232–2248. [[CrossRef](#)]

17. Rao, R.V.; Savsani, V.J.; Vakharia, D.P. Teaching-learning-based optimization: A novel method for constrained mechanical design optimization problems. *CAD Comput. Aided Des.* **2011**, *43*, 303–315. [[CrossRef](#)]
18. Goldberg, D.E.; Holland, J.H. Genetic Algorithms and Machine Learning. *Mach. Learn.* **1988**, *19* (Suppl. 2), 95–99. [[CrossRef](#)]

**Disclaimer/Publisher's Note:** The statements, opinions and data contained in all publications are solely those of the individual author(s) and contributor(s) and not of MDPI and/or the editor(s). MDPI and/or the editor(s) disclaim responsibility for any injury to people or property resulting from any ideas, methods, instructions or products referred to in the content.